Petroleum Science (2018) 15:613–624
https://doi.org/10.1007/s12182-018-0246-x

ORIGINAL PAPER

Aquathermolysis of heavy crude oil with ferric oleate catalyst

Yun-Rui Li[1] · Qiu-Ye Li[1] · Xiao-Dong Wang[1] · Lai-Gui Yu[1] · Jian-Jun Yang[1]

Received: 28 November 2017 / Published online: 17 July 2018

Abstract
Oil-soluble catalysts could be of special significance for reducing the viscosity of heavy crude oil, because of their good dispersion in crude oil and high catalytic efficiency toward aquathermolysis. Ferric oleate was synthesized and applied as catalyst in the aquathermolysis reaction of Shengli heavy oil. It was found that ferric oleate was more efficient for heavy oil cracking than Co and Ni oleates. Besides, it was superior to oleic acid and inorganic ferric nitrate and achieved the highest viscosity reduction rate of up to 86.1%. In addition, the changes in the components of Shengli heavy oil before and after aquathermolysis were investigated by elemental analysis, Fourier transform infrared spectrometry, and ^{1}H nuclear magnetic resonance spectroscopy. Results indicated that ferric oleate contributed to a significant increase in the content of light components and decrease in the content of resin, N and S. The as-prepared ferric oleate showed good activity for reducing the viscosity and improving the quality of the heavy crude oil, showing promising application potential in aquathermolysis of heavy crude oil.

Keywords Heavy oil · Viscosity reduction · Aquathermolysis · Ferric oleate · Catalyst

1 Introduction

With the excessive exploitation and rapid consumption of the conventional oil and gas resources, the exploitation of heavy crude oil and other low-grade oil and gas resources is attracting more and more attention (Huc 2010). The key issue of heavy crude oil extraction is to reduce the viscosity and increase its fluidity, and catalytic aquathermolysis could have potential for viscosity reduction in heavy crude oil (Maity et al. 2010). Early in the 1980s, Hyne and coworkers found that transition metals Ni and Co had a positive effect on the aquathermolysis of heavy oil (Chivers et al. 1980; Hyne et al. 1982). Clark et al. (1987, 1983) used thiophene and tetrahydrothiophene as the model compounds and studied the influence of transition metals on the hydrothermal cracking of heavy crude oil, and they found that group VIII transition metals contributed to significantly enhancing the desulfurization of heavy crude oil. Chen et al. (2010; 2013) proposed seven possible mechanisms to explain the viscosity reduction in heavy oil by aquathermolysis. These include hydrogenation, pyrolysis, depolymerization, isomerization, ring-opening, esterification, reconstruction and oxygenation. Needless to say, the selection of proper aquathermolysis catalysts is essential for achieving efficient hydrothermal cracking of heavy crude oil. The frequently used aquathermolysis catalysts mainly include water-soluble catalysts, oil-soluble catalysts, dispersed catalysts and solid acid catalysts (Maity et al. 2010). Among them, the oil-soluble catalysts often exhibit a high efficiency, because they can be uniformly dispersed in oil to promote the catalytic aquathermolysis reaction.

In recent years, iron-based oil-soluble catalysts have been extensively studied due to their being environment-friendly, lower cost and high efficiency. It has been found that iron naphthenate (Fan et al. 2006) is able to decrease the content of heavy components, thereby effectively reducing the viscosity of the heavy crude oil produced at Shengli Oilfield (Dongying, China). Besides, iron(III) tris(acetylacetonate) complex (Galukhin et al. 2015) catalyst can promote the transformation of high-molecular-weight components of heavy crude oil at an elevated temperature of 250 °C and an initial pressure of 3 MPa,

Edited by Xiu-Qin Zhu

✉ Qiu-Ye Li
qiuyeli@henu.edu.cn

✉ Jian-Jun Yang
yangjianjun@henu.edu.cn

[1] Engineering Research Center for Nanomaterials, Henan University, Kaifeng 475004, China

thereby significantly reducing the viscosity. Moreover, some researchers found that long-chain aromatic sulfonic iron (Wang et al. 2010; Li et al. 2013) can promote the aquathermolysis of heavy crude oil. These iron-based oil-soluble catalysts play the catalytic role of the transition metal and emulsification of organic ligands. But the reported system needs to introduce another surfactant in order to improve the contact between the catalyst and heavy oil.

Through a literature search, we found that the oleic acid ligand possessed good contact with heavy oil (Jeon et al. 2011). It has been reported that nickel oleate, cobalt oleate and molybdenum oleate (Chen et al. 2010; Wen et al. 2007) had been used to reduce the viscosity of Liaohe heavy oil and could achieve a good catalytic effect. In addition, ferric oleate (Peng 2014) exhibited efficiency for the viscosity reduction in Liaohe heavy crude oil by catalytic upgrading at 350–400 °C. However, the high temperature is unfavorable for maintaining stable catalytic efficiency and it effectively reduces production, as well as increasing the cost. Therefore, it is more meaningful to study the catalytic performance at a lower temperature.

In this study, the ferric oleate was prepared and used for the aquathermolysis of the Shengli heavy crude oil at a lower temperature. The ferric oleate exhibited higher activity than either nickel oleate or cobalt oleate. And the viscosity reduction rate of the heavy crude oil sample was up to 86.1% at a mass fraction of 10 wt%. The heavy crude oil samples before and after aquathermolysis were studied in detail by saturate, aromatic, resin and asphaltene (SARA), EL, ^{1}H-NMR, FT-IR examination and water contact angles. We also investigated the reaction mechanism of the ferric oleate.

2 Experimental section

2.1 Synthesis and characterization of ferric oleate

Excessive iron(III) nitrate nonahydrate was dissolved in distilled water to form a saturated solution in a flask. NaOH aqueous solution (1 mol/L) was slowly added into the resultant saturated solution under continuous stirring until the pH value of the mixture solution reached 4–6, followed by the addition of oleic acid at an oleic acid/ferric nitrate molar ratio of 1.8:1. The reactants were heated to 120 °C and stirred for 3 h to allow the completion of reaction. At the end of the reaction, the upper organic layer was separated using a funnel and washed three times with *n*-heptane, and then vacuum dried at 70 °C for 24 h. After the solvent was evaporated, the final product ferric oleate, a reddish-brown viscous oil, was obtained. Nickel oleate and cobalt oleate for comparative studies were synthesized in the same manner with nickel nitrate and cobalt chloride hexahydrate as the metal sources.

The as-synthesized ferric oleate catalyst was dissolved in $CHCl_3$ solution and spread evenly on a KBr pellet to form a thin film. The resultant thin film of ferric oleate was characterized by Fourier transform infrared spectrometry (FT-IR; VERTEX 70, Bruker Optics). The thermal stability of the as-synthesized ferric oleate catalyst was determined by thermogravimetric analysis (TGA, METTLER TOLEDO, TGA/SDTA851e) in air (heating rate: 10 °C/min; up to 1000 °C). The metal content of the as-synthesized ferric oleate was measured by inductively coupled plasma-atomic emission spectrometry (ICP-AES, PerkinElmer, Optima 2100DV). The carbon and hydrogen content was determined by Elemental Analyzer (EA, vario EL cube).

2.2 Catalytic aquathermolysis reaction of heavy crude oil

The heavy oil used for this research was the 3# heavy crude oil from Shengli Oilfield, China. Its properties and composition are given in Table 1. The aquathermolysis of the heavy crude oil was conducted at 200 °C for 24 h. Briefly, 50 g of the heavy crude oil was mixed with different dosages of the as-synthesized ferric oleate catalyst in an autoclave; the resultant mixture was then heated to 200 °C and held for 24 h. (The catalyst does not contain water, and the heavy crude oil contains only 12.0 wt% water). Upon completion of the aquathermolysis reaction, the viscosity of the oil samples was measured at 50 °C with a viscometer (Brookfield-DV-III). Five repeat aquathermolysis reactions were conducted for each oil sample, and the averaged

Table 1 The properties and composition of the heavy oil sample

Properties	3# Oil sample
Viscosity, mPa s	173,400
Density at 20 °C, g/cm^3	0.9834
Water content, wt%	12.0
Group composition, wt%	
Saturates	31.1
Aromatics	32.7
Resin	32.7
Asphaltene	3.5
Element content, wt%	
N	0.82
C	84.04
H	12.54
S	2.59
N_H/N_C	1.79

viscosity data are reported in this article. The viscosity reduction ratio is calculated as $\Delta\eta = (\eta_0 - \eta)/\eta_0 \times 100\%$ ($\Delta\eta$, η_0 and η are the viscosity reduction rate, the viscosity of the heavy crude oil before and after aquathermolysis reaction).

2.3 Characterization of oil samples

2.3.1 Separation of the four-group composition in oil samples

The heavy crude oil was vacuum dried at 40–50 °C for 24 h. The four-group SARA compositions of the oil samples were separated with γ-Al_2O_3 column chromatography, by the China petroleum standard method (NB/SH/T 0509-2010). The flow diagram for the separation is illustrated in Fig. 1.

2.3.2 Elemental analysis

The elemental composition (C, H, N and S) of the heavy crude oils before and after aquathermolysis and their four-group composition (saturated, aromatic, resin and asphaltene; denoted as SARA) were determined by elemental analysis (EA, Elemental Analyzer vario EL cube).

2.3.3 Fourier transform infrared spectroscopy

The oil samples and their heavy components (resin and asphaltene) before and after aquathermolysis were dissolved in CCl_4 and spread evenly on KBr pellets to form a thin film after solvent evaporation for FT-IR spectroscopy.

2.3.4 ^{1}H NMR

The ^{1}H NMR spectra of oil samples and heavy component (resin and asphaltene) before and after reaction were recorded on an Avance III HD 400 MHZ, and $CDCl_3$ was used as the solvent (with TMS as the internal reference material).

2.3.5 Water contact angle

A contact angle meter (Kruss, DSA100S) was employed to determine the water contact angles of the heavy crude oil with ferric oleate.

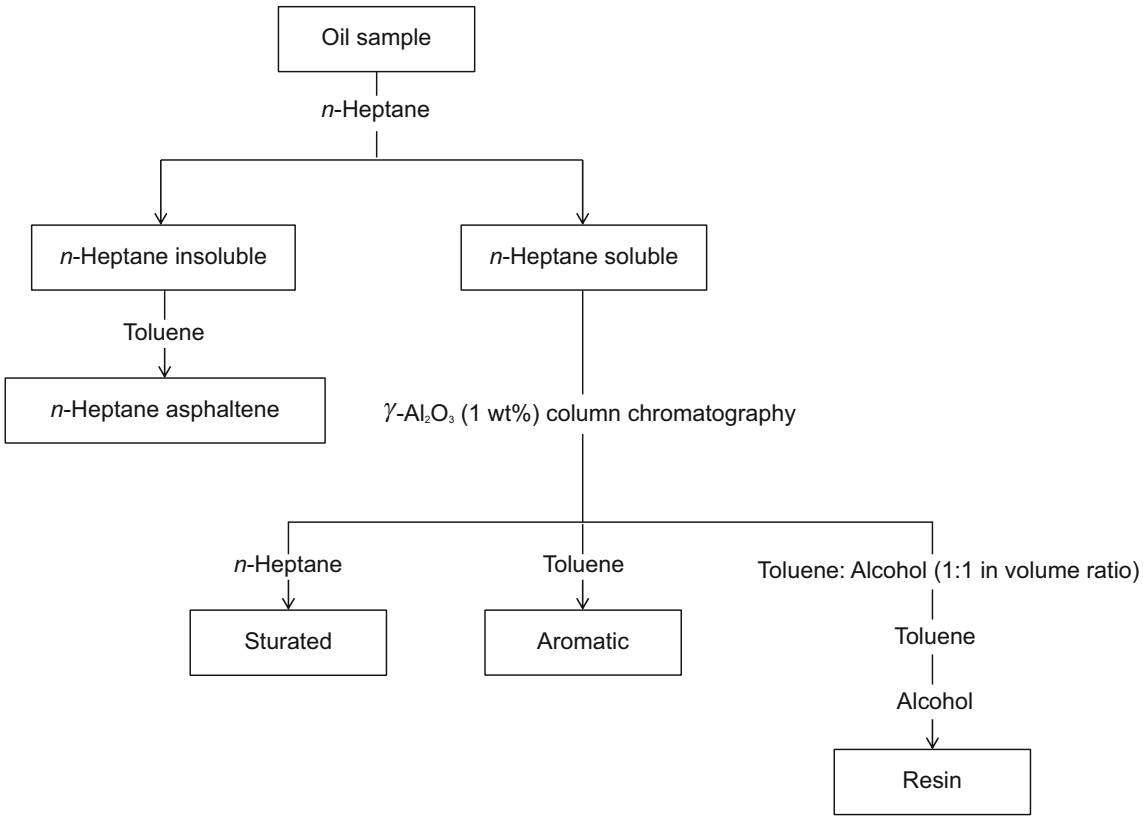

Fig. 1 The flow diagram for the separation of four-group composition in oil sample

3 Results and discussion

3.1 Characterization of ferric oleate

The FT-IR spectra of oleic acid and ferric oleate are shown in Fig. 2. Ferric oleate exhibits characteristic absorbance peaks of $\nu(COO^-)$ at 1711, 1592, 1458, and 1419 cm^{-1}. The characteristic peaks of metal carboxylates are in the range of 1610–1540 cm^{-1} for the antisymmetric stretching vibration and 1464–1360 cm^{-1} for the symmetric stretching vibration. (The latter was often split into two or three broad peaks.) The peak at 1711 cm^{-1} is assigned either to the symmetric stretching vibration of free oleic acid or to the asymmetrical stretching vibration of unidentate carboxylate. The absorption peak at 733–723 cm^{-1} is assigned to the $-(CH_2)_n-$ ($n \geq 4$) of the long-alkyl side chain of the catalyst (Bronstein et al. 2007; Palchoudhury et al. 2011). Moreover, the coordination modes of the metal carboxylate can be deduced by the frequency difference between the antisymmetric and symmetric stretching vibration of $\nu(COO^-)$, Δ, in the range of 1300–1700 cm^{-1}. In this research, it could be deduced that the iron carboxylate is iron-coordinated or bridging-coordinated, because Δ= 134 cm^{-1} ($110 < \Delta < 200$ cm^{-1}) (Palchoudhury et al. 2011). Therefore, the ferric oleate catalyst was prepared successfully.

The TGA/DTG curves of the as-synthesized ferric oleate and oleic acid are shown in Fig. 3a. The mass loss in the range of 150–292 °C (Fig. 3a, region a) is due to the dissociation of two oleate ligands from ferric oleate, and the mass loss at 292–354 °C (Fig. 3a, region b) is due to the dissociation of the remaining one oleate ligand, and the DTG curve peak areas ratio of the two mass loss region is close to 2:1 (Palchoudhury et al. 2011). The mass loss at ~ 354 °C is due to desorption of decomposed oleic acid ligands and evaporation of remaining organic components (Fig. 3a, region c). The weight loss in the range of 356–389 °C (Fig. 3a, region c) might be due to the decomposition of impurity ferric nitrate (Shanmugam et al. 2003). The trace weight loss around 100 °C is derived from the evaporation of solvent. The results of thermogravimetry analysis are indicated that there are three oleic acid ligands on an iron ion.

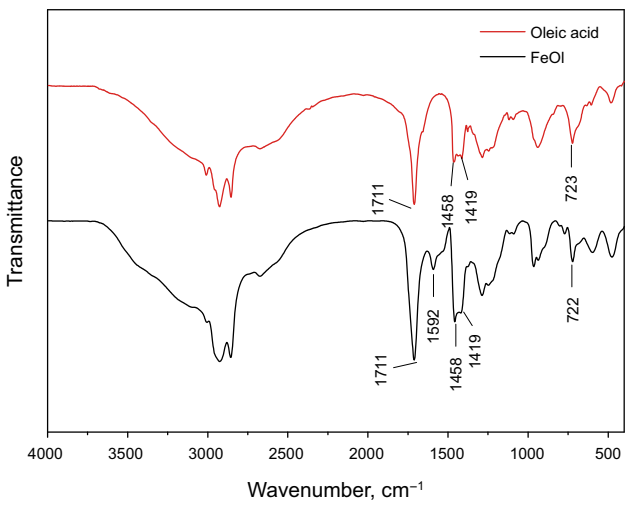

Fig. 2 FT-IR spectra of oleic acid and ferric oleate (FeOl)

The elemental analysis (C, H) and ICP data (Fe) of the as-synthesized catalyst are shown in Table 2. The results show that the C/H ratio of catalyst we synthesized is close to the theoretical structure of $Fe(oleate)_3$. And the residual value calculated by theory is 10.4 wt%, which is close to 14.8 wt% that obtained from the TGA/DTG curve (Fig. 3a). Based on the results of FT-IR and TGA/DTG analysis, we can infer that ferric oleate exhibits an iron-coordination mode. The molecular structure of ferric oleate is shown in Fig. 4.

In combination with the TGA/DTG curve of oleic acid in Fig. 3b, we can, therefore, draw the conclusion that ferric oleate has good thermal stability and has promising applications as an aquathermolysis catalyst. The long-chain structure of the oleate catalyst is helpful to enhance the contact with heavy crude oil, thereby improving the aquathermolysis catalytic efficiency.

Nickel oleate and cobalt oleate prepared in the same manner also exhibit good thermal stability (Their FT-IR spectra and TGA/DTG curves are presented in Figs. 5 and 6). Namely, the oleic ligand of nickel oleate and cobalt oleate is stable at 200 °C, which means that they could be potential moderate-temperature aquathermolysis catalysts for heavy crude oil.

3.2 Catalytic aquathermolysis of heavy crude oil

3.2.1 Effect of different oleates on the aquathermolysis of heavy crude oil

Three different oleate catalysts (ferric oleate, nickel oleate and cobalt oleate) were used to catalyze the aquathermolysis reaction of the heavy crude oil, and the dosage of the catalyst was fixed at 1.0 wt% (mass fraction; the same hereafter). As shown in Fig. 7, the viscosity reduction ratio without catalyst was 19.0%, due to the thermal cracking of the heavy crude oil. When ferric oleate, nickel oleate and cobalt oleate were separately introduced into the heavy crude oil, the viscosity reduction ratio was 34.0, 24.3, and 3.3%, respectively. Ferric oleate had the best performance in reducing the viscosity of the heavy crude oil, because it contains three oleic acid ligands and exhibited good dispersion and contact with the heavy crude oil. In addition, cobalt can be associated with the heavy components of the heavy crude oil at high temperature, and this accounts for

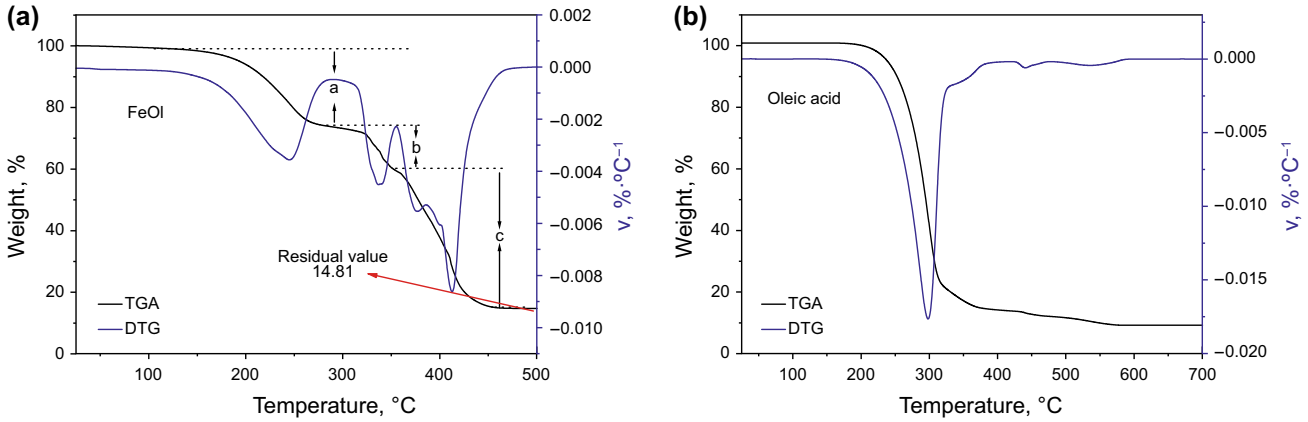

Fig. 3 TGA/DTG curves of ferric oleate (**a**) and oleic acid (**b**)

Table 2 Elemental (C, H, Fe) analysis data of the synthesized catalysts

Sample	C, wt%	H, wt%	Fe, wt%	N_C/N_H	N, wt%
Ferric oleate (FeOl)	61.64	9.12	10.01	0.56	0.43
[a]$Fe(oleate)_3$	[a]72.08	[a]11.01	[a]6.23	0.55	0

[a]The theoretical C, H, Fe content of ferric oleate

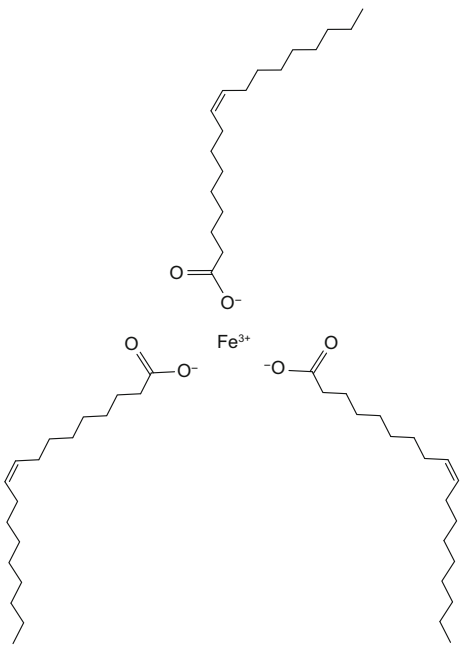

Fig. 4 Molecular structure of ferric oleate (FeOl)

its poorest viscosity-reduction ability among the three oleate catalysts (Hong et al. 2001).

In order to study the effect of Fe^{3+} and the long-alkyl chain of the ferric oleate catalyst on the aquathermolysis of

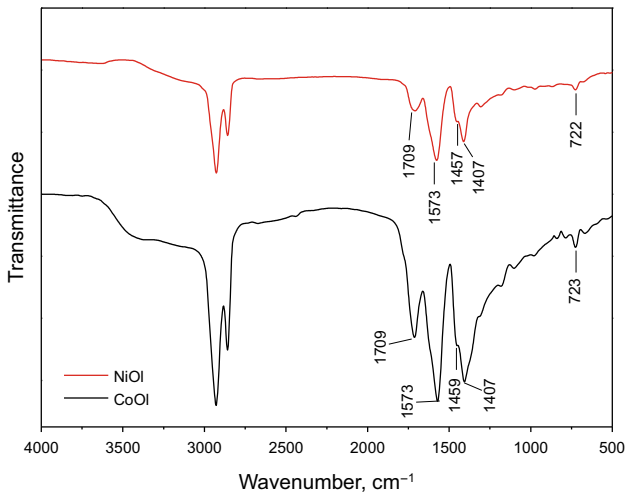

Fig. 5 FT-IR spectra of nickel oleate (NiOl) and cobalt oleate (CoOl)

the heavy crude oil, we selected water-soluble iron nitrate nonahydrate and oleic acid as the reference and conducted comparative experiments at a catalyst dosage of 0.50 wt% (ferric oleate), 0.45 wt% (oleic acid) and 0.35 wt% (nonahydrate iron nitrate), respectively. (The catalyst dosage is calculated based on the content of Fe listed in Table 2.) As shown in Fig. 8, ferric oleate exhibits a much higher viscosity reduction ratio than oleic acid. The viscosity of the heavy crude oil is reduced after aquathermolysis in the presence of oleic acid, which could be due to the dilution and emulsification function of oleic acid. (Oleic acid can reduce the water surface tension to 42.49 mN/m.) Ferric oleate contributes significantly to the viscosity reduction in the heavy crude oil. This is because, on the one hand, Fe^{3+} can catalyze the aquathermolysis of the heavy crude oil well; on the other hand, the long-alkyl chain exhibits an emulsification function (ferric oleate can reduce the water surface tension to 33.82 mN/m), thereby showing greatly increased viscosity-reduction ability. In contrast to oleic acid and ferric oleate, iron nitrate nonahydrate leads to an

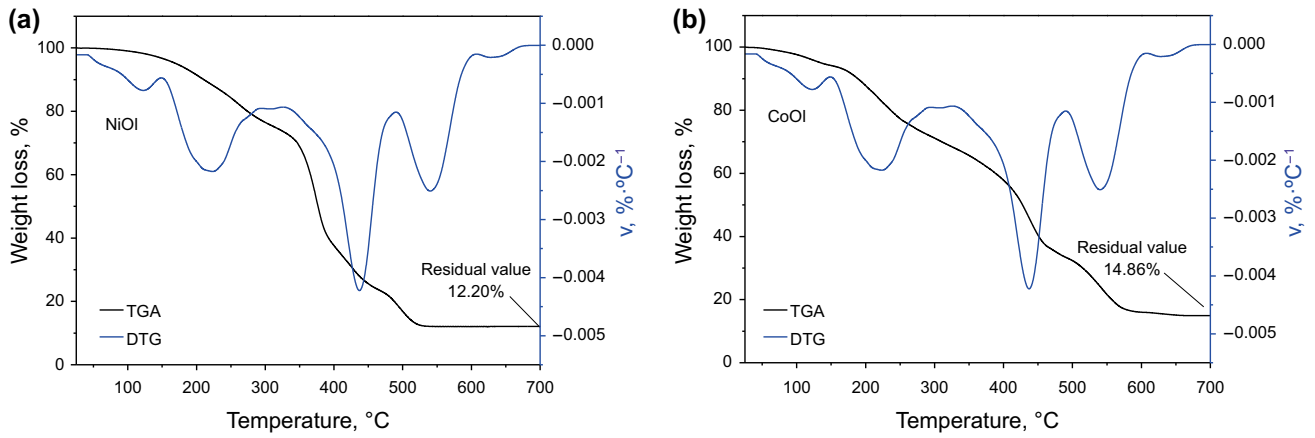

Fig. 6 TGA/DTG curves of nickel oleate (**a**) and cobalt oleate (**b**)

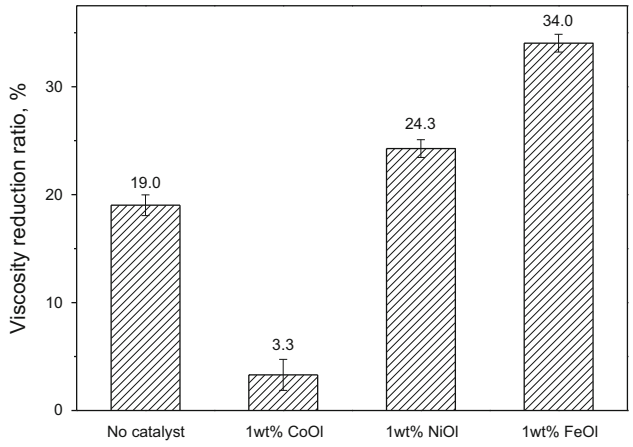

Fig. 7 Viscosity reduction ratios of Fe, Ni and Co oleates

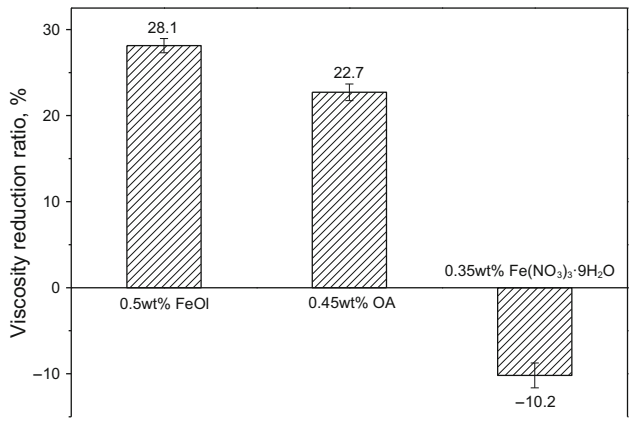

Fig. 8 Viscosity reduction ratios with ferric oleate, oleic acid and iron (III) nitrate nonahydrate

increase in the viscosity of the heavy crude oil. This could be because, under the catalytic role of iron nitrate, the high content of nitrogen could promote the polymerization of the heavy components and give rise to coke, thereby inhibiting the thermal cracking reaction and increasing the viscosity (Liang 2003).

In addition, the different catalysts containing short chain acids (lauric acid, myristic acid, oleic acid) are illustrated in Fig. 9 of the supporting information. Through comparison of the viscosity reduction ratio of the three different organic acids, we found that the oleic acid exhibited the best activity.

3.2.2 Effect of ferric oleate dosage on the viscosity of heavy crude oil

As shown in Fig. 10, the dosage of ferric oleate has a great effect on the viscosity change of the heavy crude oil. The viscosity reduction ratio increases gradually with the increase in ferric oleate dosage. The highest viscosity reduction ratio (up to 86.1%) is achieved at a ferric oleate dosage of 10.0 wt%.

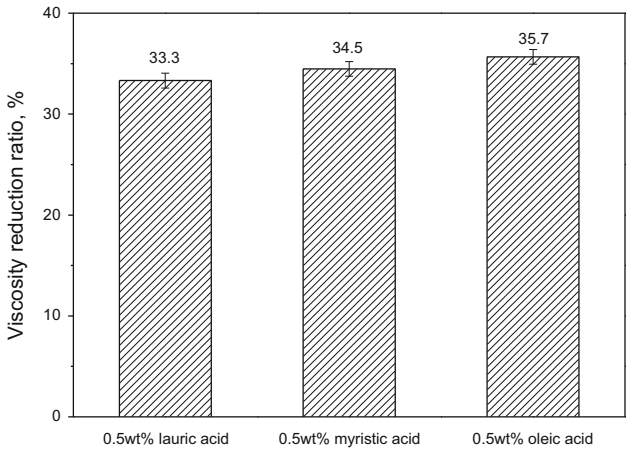

Fig. 9 The viscosity reduction ratio of oleic acid, myristic acid and lauric acid (the heavy oil used for this research from the 4# oil at Shengli Oilfield, and the viscosity of the crude oil was measured to be 171,900 mPa s at 50 °C)

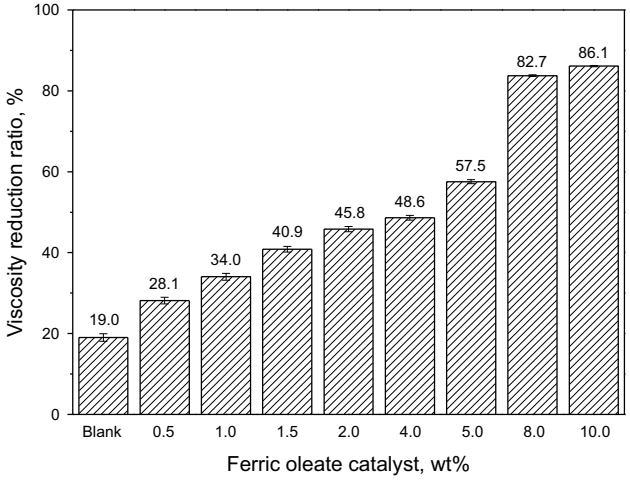

Fig. 10 Viscosity reduction ratios with different mass ratios of ferric oleate catalyst

3.3 The change of properties before and after aquathermolysis

3.3.1 Analysis of SARA components

In consideration of the efficiency and economy, the reaction system with 8.0 wt% FeOl was selected to analyze the components of the heavy crude oil before and after aquathermolysis. The SARA components of the heavy crude oil samples are listed in Table 3. After aquathermolysis in the presence of ferric oleate, the content of the SARA components changes greatly. Namely, the content of light components increases and heavy components decrease after the aquathermolysis. This indicates that ferric oleate can promote the transformation of heavy components into light components. Besides, the content of resin decreases and the content of asphaltene increases after the aquathermolysis reaction in the presence of ferric oleate. Resin could help to promote the dispersion of asphaltene particles in heavy crude oil (Bhardwaj and Hartland 1994), and further, the ratio between resin and asphaltene could affect the stability of asphaltene (Li et al. 1999; Mansoori 1997). As listed in Table 4, the ratio of resin and asphaltene decreases after aquathermolysis in the presence of ferric oleate catalyst. This means that, during the aquathermolysis reaction, ferric oleate catalyst can promote the association and coalescence of macromolecules in asphaltene.

Table 4 Ratios between saturates and aromatic as well as resin and asphaltene before and after aquathermolysis reaction

Sample	3# Oil sample	Oil after reaction
Saturated (%)/Aromatic (%)	0.95	0.95
Resin (%)/Asphaltene (%)	9.39	6.79

3.3.2 Element analysis of heavy crude oil as well as its heavy components

The C, H, N, S elemental content of the heavy oil and its heavy components (resin and asphaltene) before and after aquathermolysis are listed in Table 5. After the aquathermolysis reaction, the ratio of N_H/N_C (H/C ratio, the atomic ratio of hydrogen to carbon) of the heavy crude oil increases from 1.79 to 1.94; the heteroatoms amount of N decreases from 0.82 to 0.77, and the content of S decreases from 2.59 to 2.36. This indicates that the breaking of C-S and C-N bonds may have happened during the hydrocracking reaction. As to the heavy components, the N content in the resin and asphaltene remains unchanged after the aquathermolysis reaction, and that of S decreases a little. This indicates that ferric oleate has a small effect on the desulfurization of the heavy components.

3.3.3 FT-IR analysis of heavy components before and after aquathermolysis

Figure 11 shows the FT-IR spectra of resin and asphaltene of the heavy crude oil before and after aquathermolysis. The assignments of the infrared absorbance peaks are summarized in Table 6. As to resin, the absorbance peak at 732 cm^{-1} is weakened and moved to a lower wavenumber region (728 cm^{-1}) after the aquathermolysis reaction (Fig. 11a), possibly due to the destruction of the long side chain generating shorter chains. The peaks in the wavenumber range of 800–840 cm^{-1} (871, 822 and 748 cm^{-1}) demonstrate that substitution products could be generated after the aquathermolysis reaction. Besides, as shown in Fig. 11b, ferric oleate catalyst has nearly no

Table 3 SARA components of 3# heavy crude oil sample before and after aquathermolysis with FeOl

Oil sample	Saturate, wt%	Aromatic, wt%	Light component, wt%	Resin, wt%	Asphaltene, wt%	Heavy component, wt%
3# Oil sample	31.1	32.8	63.8	32.7	3.5	36.2
Oil after reaction	32.1	33.8	66.0	29.7	4.4	34.0

Table 5 Element compositions of heavy crude oil and its heavy components before and after aquathermolysis

Sample	N, wt%	C, wt%	H, wt%	S, wt%	N_H/N_C
3# Oil sample	0.82	84.04	12.54	2.59	1.79
Oil sample after reaction with ferric oleate	0.77	83.42	13.45	2.36	1.94
Resin before reaction	1.38	84.71	10.74	3.17	1.52
Resin after reaction with ferric oleate	1.38	84.72	10.85	3.06	1.54
Asphaltene before reaction	1.66	84.40	10.03	3.91	1.42
Asphaltene after reaction with ferric oleate	1.66	85.09	9.70	3.52	1.37

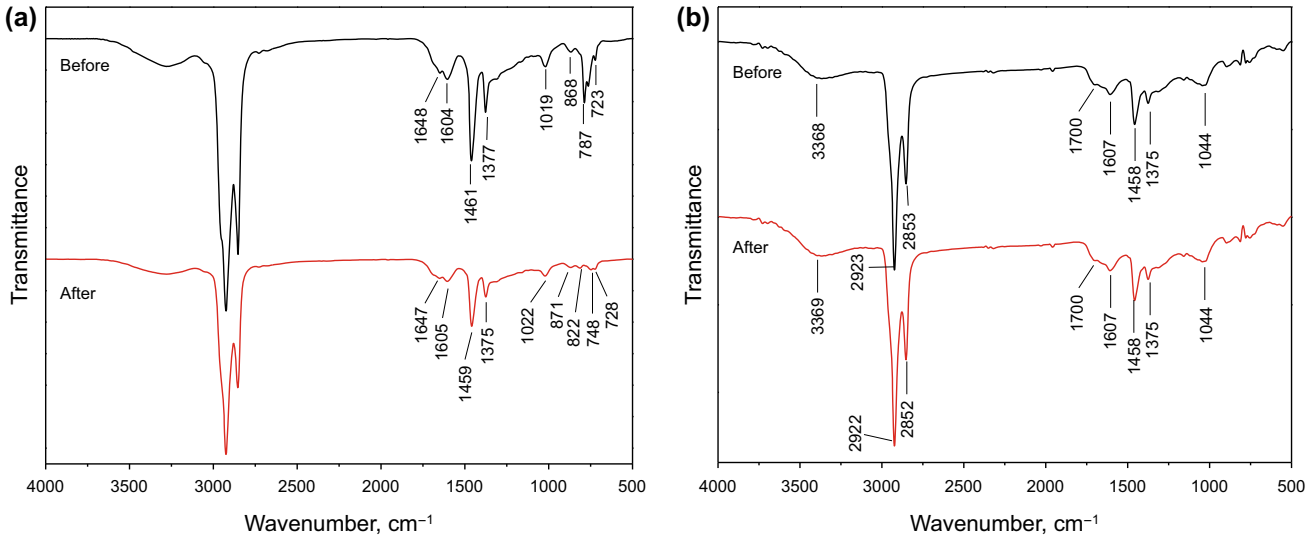

Fig. 11 FT-IR spectra of the resin (**a**) and asphaltene (**b**) before and after the reaction

Table 6 FT-IR absorbance peaks of resin and asphaltene components

Wavenumbers, cm^{-1}	Infrared absorption characteristic peaks and the vibrations forms
3500–3300	$-NH_2$ or free −NH, stretching vibration
2933–2923, 2860–2840	$-CH_2$, symmetric and antisymmetric vibrations
1680–1620	C=C, stretching vibration
1850–1600	−C=O (alcohols, aldehydes, acid and ketones, etc.), stretching vibration
1470–1450	$-CH_3$, $-CH_2$, deformation vibration
1608, 1460	Asymmetric stretching vibration of framework phenyl rings C=C
1380–1370	$-CH_3$, symmetrical deformation vibration
1300–1000	C−O, stretching vibration
733–723	$-(CH_2)_n-$, $n \geq 4$
800–600	C–Cl

effect on the content of asphaltene after the aquathermolysis reaction. This is consistent with corresponding SARA data and element analysis data. According to Eq. (1), the side chain length of resin and asphaltene can be estimated from the n_{CH2}/n_{CH3} ratio determined by FT-IR. In Eq. (1), n_{CH2} and n_{CH3} represent the number of methylene and methyl, and S_{1460} and S_{1380} are the feature peak area of IR spectra at 1460 and 1380 cm^{-1} (Liang et al. 1987). As listed in Table 7, the n_{CH2}/n_{CH3} ratio of resin tends to decrease after the aquathermolysis reaction, which proves that the side chains can be cracked by the aquathermolysis reaction.

$$n_{CH3}/n_{CH3} = 4.00S_{1460}/S_{1380} - 13.80 \quad (1)$$

3.3.4 ^{1}H-NMR analysis of heavy crude oil samples as well as their resin and asphaltene components

The ^{1}H-NMR spectra of oil samples, resin and asphaltene before and after reaction were shown in Fig. 12, and the

Table 7 The n_{CH2}/n_{CH3} ratio of resin and asphaltene before and after aquathermolysis

Sample	S_{1460}/S_{1380}	n_{CH2}/n_{CH3}
Resin before reaction	4.190	2.940
Resin after reaction with ferric oleate	4.058	2.412
Asphaltene before reaction	4.712	5.028
Asphaltene after reaction with ferric oleate	4.711	5.024

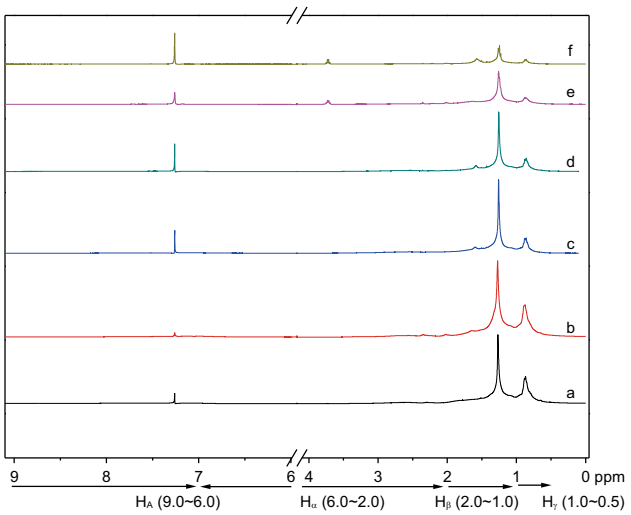

Fig. 12 ^{1}H NMR spectra of oil samples, resins and asphaltenes before and after reaction. **a** ^{1}H NMR spectra of oil sample before reaction, **b** ^{1}H NMR spectra of oil sample after reaction, **c** ^{1}H NMR spectra of resin before reaction, **d** ^{1}H NMR spectra of resin after reaction, **e** ^{1}H NMR spectra of asphaltene before reaction, **f** ^{1}H NMR spectra of asphaltene after reaction)

assignments in the ^{1}H NMR chemical shifts were shown in Table 8. The ^{1}H-NMR data (H_A, H_α, H_β, H_γ) of the heavy crude oil samples as well as their resin and asphaltene components before and after aquathermolysis reaction are shown in Table 9. The parameters such as the aromaticity factor (f_A), aromaticity condensation (H_{AU}/C_A), replacement rate of periphery hydrogen in the aromatic ring system (σ) and branchiness index (BI) were calculated by Eqs. (2)–(5), respectively (Liang et al. 1991):

$$f_A = \frac{C_T/H_T - (H_\alpha + H_\beta + H_\gamma)/2H_T}{C_T/H_T} \quad (2)$$

$$\frac{H_{AU}}{C_A} = \frac{H_A/H_T + H_\alpha/2H_T}{C_T/H_T - (H_\alpha + H_\beta + H_\gamma)/2H_T} \quad (3)$$

$$\sigma = \frac{H_\alpha/2}{H_A + H_\alpha/2} \quad (4)$$

$$BI = \frac{\frac{1}{3}S_{CH_3}}{\frac{1}{2}S_{(CH_2+CH)}} \quad (5)$$

In Eqs. (2)–(5), C_T and H_T represent the total amounts of carbon and hydrogen, $H_T = H_A + H_\alpha + H_\beta + H_\gamma$, and C_T/H_T is the ratio of carbon to hydrogen. The value of C_T/H_T for saturated content is assumed to be 2. As seen in Eq. (3), the higher the H_{AU}/C_A value, the lower the aromaticity condensation. In the meantime, when σ value increases, the aromatic ring undergoes hydrogenation [Eq. (4)]. Moreover, the higher the BI value, the larger the degree of branching of macromolecular chains and the shorter the branch chain [Eq. (5)]. The detailed calculated results are summarized in Table 10.

As listed in Table 10, the aromaticity factor (f_A) of the heavy crude oil decreases after aquathermolysis, and the aromaticity condensation value (H_{AU}/C_A) also increases. Besides, the value (σ) of the replacement rate of periphery hydrogen in the aromatic ring system and the branchiness index (BI) increase after the aquathermolysis reaction. The decrease in the aromaticity factor indicates that the hydrogenation reaction could give rise to unsaturated components. On the contrary, the increase in the aromaticity condensation refers to a decrease in the condensation degree of the aromatic ring system as well as the occurrence of ring-opening after the aquathermolysis reaction. Moreover, the increase in the replacement rate of peripheral hydrogen in the aromatic ring system indicates that a hydrogenation reaction might occur in the aromatic ring. The increase in the branching index of the side chains indicates that the branching degree of the carbon chain increases and the side chain length decreases in association with side chain breakage after the aquathermolysis reaction.

Table 8 Assignments in the ^{1}H NMR chemical shifts

Parameter	Assignment	Chemical shift, ppm
H_A	Aromatic hydrogen	6.0–9.0
H_α	Aliphatic hydrogen attached to C_α to aromatic rings	2.0–4.0
H_β	Aliphatic hydrogen attached to C_β and the CH_2, CH beyond the C_β to aromatic rings	1.0–2.0
H_γ	Aliphatic hydrogen attached to C_γ and the CH_3 beyond the C_γ to aromatic rings	0.5–1.0

Table 9 ^{1}H NMR chemical shifts of oil samples, resin and asphaltene before and after reaction

Sample	H_A, %	H_α, %	H_β, %	H_γ, %
3# Oil sample	3.40	6.57	59.55	30.58
Oil sample after reaction with ferric oleate	4.10	8.18	56.83	30.90
Resin before reaction	2.30	13.65	62.94	21.11
Resin after reaction with ferric oleate	3.71	12.92	59.32	24.05
Asphaltene before reaction	2.30	15.01	62.91	19.78
Asphaltene after reaction with ferric oleate	2.57	18.28	59.67	19.48

Table 10 Structural parameters of heavy crude oil samples as well as their resin and asphaltene components before and after reaction

Sample	f_A	H_{AU}/C_A	σ	BI
3# Oil sample	0.135	0.884	0.491	0.307
Oil sample after reaction with ferric oleate	0.070	2.280	0.499	0.317
Resin before reaction	0.257	0.539	0.748	0.184
Resin after reaction with ferric oleate	0.259	0.606	0.635	0.222
Asphaltene before reaction	0.301	0.465	0.765	0.169
Asphaltene after reaction with ferric oleate	0.333	0.482	0.781	0.167

As to the resin component after the aquathermolysis reaction in the presence of the ferric oleate catalyst, the aromaticity condensation value increases, the value of the replacement rate of peripheral hydrogen in the aromatic ring system decreases, and the branchiness index rises. For the asphaltene component, the aromaticity condensation value and the replacement rate of the peripheral hydrogen in the aromatic ring system increase after the aquathermolysis reaction.

The above mentioned ^{1}H-NMR data indicate that the introduction of ferric oleate catalyst during the aquathermolysis reaction of the heavy crude oil contributes to promoting hydrogenation, ring-opening and side chain breakage, thereby adding to the fracturing of the heavy crude oil. Particularly, the ferric oleate catalyst contributes to the ring-opening and side chain fracturing of the resin component as well as to the aromatic ring hydrogenation reaction and polymerization of the asphaltene component. And these are consistent with corresponding FT-IR, SARA and EL analysis.

3.3.5 Water contact angle

The heavy crude oil is a water-in-oil emulsion. The contact angle was able to illustrate the emulsification (Langevin et al. 2004). Figure 13 showed the effect of ferric oleate dosage on the water contact angle of the heavy crude oil. The water contact angle of the as-received heavy crude oil without ferric oleate is 109.1°, and the addition of ferric oleate catalyst up to a dosage of 4.0 wt% leads to increases in the water contact angles. When the dosage of ferric oleate is small, the oleic acid ligands are mainly adsorbed on the surface of oil droplets to promote the catalytic reaction. After the reaction, it will adsorb on the surface of the oil droplets to increase the contact angles. The dosage of the catalyst in the dosage range of 5.0–10.0 wt%, however, causes decreases in the water contact angles of the tested heavy crude oil. Particularly, the lowest water contact angle is achieved at a ferric oleate dosage of 8.0 wt%, which corresponds to the formation of an oil-in-water (O/W) emulsion. These indicate that the catalytic reaction is predominant at a low ferric oleate dosage (below 4.0 wt%), while emulsification is predominant at a high ferric oleate dosage (above 5.0 wt%).

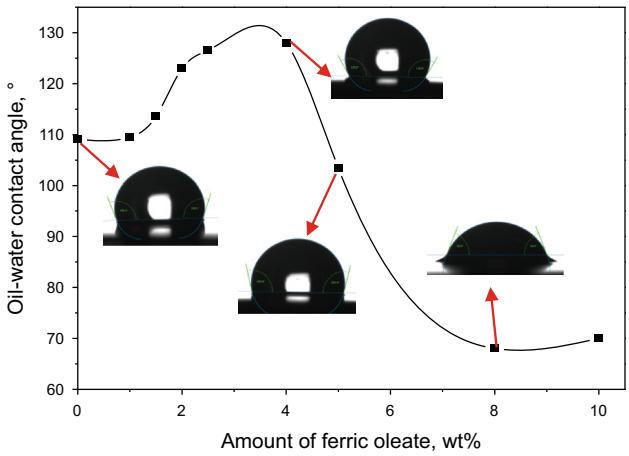

Fig. 13 Water contact angles of heavy crude oil with different contents of ferric oleate

3.4 The viscosity reduction mechanism of the heavy crude oil

In terms of the mechanism for promoting the aquathermolysis reaction of the heavy crude oil, ferric oleate

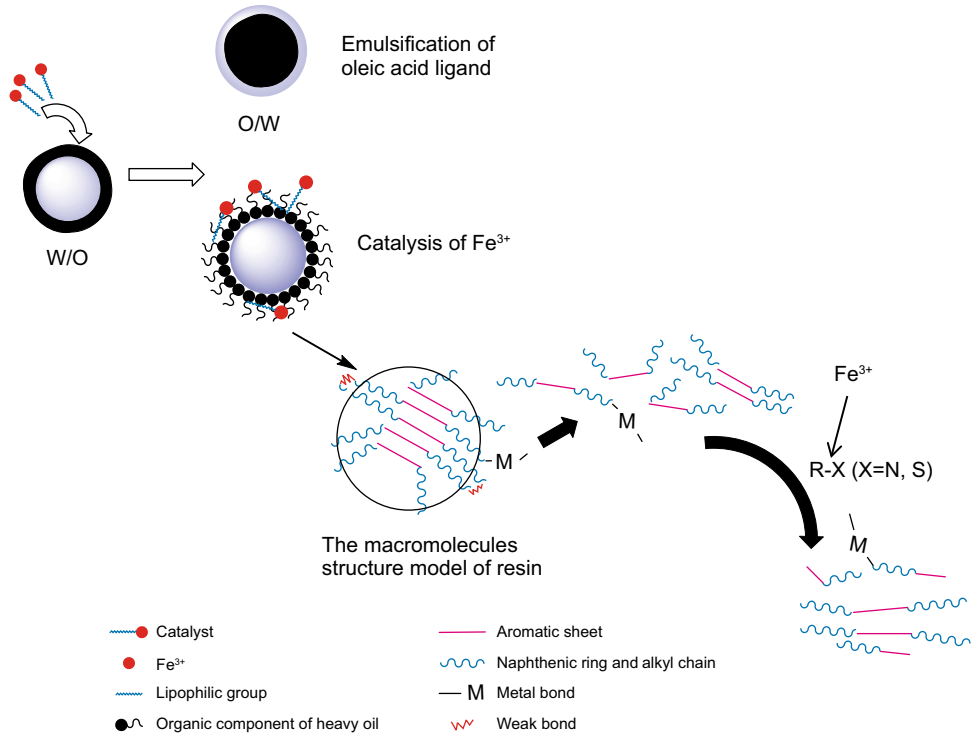

Fig. 14 Schematic diagram of action mechanism of ferric oleate catalyst

catalyst functions by the catalysis of the transition metal Fe^{3+} and the emulsification of oleic long-alkyl chains. Its action mechanism is schematically shown in Fig. 14. On one hand, the oleic acid ligand contributes to promoting the formation of an O/W emulsion and increasing the contact area of the transition metal with oil, thereby effectively enhancing the aquathermolysis reaction. On the other hand, the oleic acid ligand caused the aggregation state of the resin macromolecules to be destroyed. And Fe^{3+} contributes to promoting the hydrogenation, polymerization, ring-opening, long side chain breakage, desulfurization and denitrification of the heavy crude oil during catalytic aquathermolysis. As a result, the heavy components are more effectively transformed into light components, leading to a reduction in the viscosity and an improvement in the quality of the heavy crude oil.

4 Conclusions

In summary, three oil-soluble oleates were synthesized, and their effect on the aquathermolysis reaction of the heavy crude oil extracted at Shengli Oilfield was investigated in relation to structure characterizations as well as water contact angle measurement. Results indicate that ferric oleate is more effective in reducing viscosity than nickel and cobalt oleates. The viscosity reduction ratio increases gradually with increasing dosage of ferric oleate. Particularly, the highest viscosity reduction ratio (up to 86.1%) is achieved when the heavy crude oil is allowed to undergo aquathermolysis at 200 °C for 24 h in the presence of 10.0 wt% ferric oleate catalyst. The good ability of ferric oleate to reduce the viscosity of the heavy crude oil is attributed to the catalytic role of Fe^{3+} and the emulsification function of oleic long-alkyl chains. Such a dual function of the ferric oleate during catalytic aquathermolysis contributes to increase the contact area of transition metal with oil and promoting the hydrogenation, polymerization, ring-opening, long side chain breakage, desulfurization and denitrification of the heavy crude oil, thereby reducing the viscosity and improving the quality of the heavy crude oil.

Acknowledgements The authors gratefully acknowledge the support of the National Natural Science Foundation of China (Nos. 21471047 and 21371047) and Natural Science Foundation of Henan Province of China (162300410014).

References

Bhardwaj A, Hartland S. Kinetics of coalescence of water droplets in water-in-crude oil emulsions. J Disper Sci Tech.

1994;15(2):133–46. https://doi.org/10.1080/01932699408943549.

Bronstein LM, Huang XL, Retrum J, et al. Influence of iron oleate complex structure on iron oxide nanoparticle formation. Chem Mater. 2007;19:3624–32. https://doi.org/10.1021/cm062948j.

Chen EY, Liu YJ, Liang M, et al. A study on the viscosity reduction of Liaohe heavy oil by oil soluble nickel oleate. J Daqing Pet Inst. 2010;34(6):68–71. https://doi.org/10.3969/j.issn.2095-4107.2010.06.012.

Chivers T, Hyne JB, Lau C. The thermal decomposition of hydrogen sulfide over transition metal sulfides. Int J Hydrog Energy. 1980;5(5):499–506. https://doi.org/10.1016/0360-3199(80)90056-7.

Clark PD, Dowling NI, Lesage KL, et al. Chemistry of organosulphur compound types occurring in heavy oil sands: 5. Reaction of thiophene and tetrahydrothiophene with aqueous Group VIIIB metal species at high temperature. Fuel. 1987;66(12):1699–702. https://doi.org/10.1016/0016-2361(87)90366-8.

Clark PD, Hyne JB, Tyrer JD. Chemistry of organosulfur compound types occurring in heavy oil sands: 1. High temperature hydrolysis and thermolysis of tetrahydrothiophene in relation to steam stimulation processes. Fuel. 1983;62(8):959–62. https://doi.org/10.1016/0016-2361(83)90170-9.

Fan ZX, Zhao FL, Wang JX, et al. Upgrading and viscosity reduction of super heavy oil by aquathermolysis with hydrogen donor. J Fuel Chem Tech. 2006. https://doi.org/10.3969/j.issn.0253-2409.2006.03.011.

Galukhin AV, Erokhin AA, Osin YN, et al. Catalytic aquathermolysis of heavy oil with Iron Tris(acetylacetonate): changes of heavy oil composition and in situ formation of magnetic nanoparticles. Energy Fuels. 2015;29(8):4768–73. https://doi.org/10.1021/acs.energyfuels.5b00587.

Hong FF, Yong JL, Li GZ. Studies on the synergetic effects of mineral and steam on the composition changes of heavy oil. Energy Fuels. 2001;15(6):1475–9. https://doi.org/10.1021/ef0100911.

Huc AY. Heavy Crude Oils; From geology to upgrading, an overview. Paris: Technip; 2010. https://www.researchgate.net/publication/263818045.

Hyne JB, Clark PD, Clarke RA, et al. Aquathermolysis of heavy oils. In: Proceedings of the 2nd international conference on heavy crude and tar sands; 1982; Caracas, Venezuela. https://www.researchgate.net/publication/284792867.

Jeon SG, Na JG, Ko CH, et al. Preparation and application of an oil-soluble CoMo bimetallic catalyst for the hydrocracking of oil sands bitumen. Energy Fuels. 2011;25(10):4256–60. https://doi.org/10.1021/ef200703t.

Langevin D, Poteau S, Hénaut I, et al. Crude oil emulsion properties and their application to heavy oil transportation. Oil Gas Sci Technol. 2004;59:511–21. https://doi.org/10.2516/ogst:2004036.

Li J, Chen Y, Liu H, et al. Influences on the aquathermolysis of heavy oil catalyzed by two different catalytic ions: Cu^{2+} and Fe^{3+}. Energy Fuels. 2013;27(5):2555–62. https://doi.org/10.1021/ef400328s.

Li S, Liu C, Que G, et al. Colloidal structures of vacuum residua and their thermal stability in terms of saturate, aromatic, resin and asphaltene composition. J Pet Sci Eng. 1999;22:37–45. https://doi.org/10.1016/s0920-4105(98)00055-2.

Liang WJ. Heavy oil chemistry. Shandong: China University of Petroleum; 2003.

Liang WJ, Han SQ, Liu WQ. Determination of ratio of methylene and methyl in paraffinic hydrocarbons with infrared spectroscopy. Journal of East China Petroleum Institute. 1987;11(2): 86–90. http://www.wanfangdata.com.cn/details/detail.do?_type=perio&id=QK000002987543.

Liang WJ, Que GH, Chen YZ. Chemical composition and structure of vacuum residues of Chinese crudes II. Average structure of vacuum residues and their fractions. Acta Pet Sin: Pet Process Sect. 1991;7(4):1–11. http://www.wanfangdata.com.cn/details/detail.do?_type=perio&id=QK000002922969.

Maity SK, Ancheyta J, Marroquín G, et al. Catalytic aquathermolysis used for viscosity reduction of heavy crude oils: a review. Energy Fuels. 2010;24(5):2809–16. https://doi.org/10.1021/ef100230k

Mansoori GA. Modeling of asphaltene and other heavy organic depositions. J Pet Sci Eng. 1997;17:101–11. https://doi.org/10.1016/s0920-4105(96)00059-9.

Palchoudhury S, An W, Xu Y, et al. Synthesis and growth mechanism of iron oxide nanowhiskers. Nano Lett. 2011;11(3):1141–6. https://doi.org/10.1021/nl200136j.

Peng X. Experimental study on visbreaking of heavy oil by catalytic upgrading. J Chongqing Univ Sci Technol Nat Sci Ed. 2014;16(5):20–3. https://doi.org/10.3969/j.issn.1673-1980.2014.05.006.

Shanmugam Y, Lin FY, Chang TH, et al. Thermal decomposition of metal nitrates in air and hydrogen environments. J Phys Chem B. 2003;107:1044–7. https://doi.org/10.1021/jp026961c.

Wang YQ, Chen YL, He J, et al. Mechanism of catalytic aquathermolysis: influences on heavy oil by two types of efficient catalytic ions: $Fe^{3+}$and Mo^{6+}. Energy Fuels. 2010;24(3):1502–10. https://doi.org/10.1021/ef901339k.

Wen SB, Zhao YJ, Liu YJ, et al. A study on catalytic aquathermolysis of heavy crude oil during steam stimulation. Soc Pet Eng. 2007;3:1–5. https://doi.org/10.2523/106180-ms.